Cell Stem Cell, Volume *29*

Supplemental Information

SARS-CoV-2 infects the human kidney and drives fibrosis in kidney organoids

Jitske Jansen, Katharina C. Reimer, James S. Nagai, Finny S. Varghese, Gijs J. Overheul, Marit de Beer, Rona Roverts, Deniz Daviran, Liline A.S. Fermin, Brigith Willemsen, Marcel Beukenboom, Sonja Djudjaj, Saskia von Stillfried, Larissa E. van Eijk, Mirjam Mastik, Marian Bulthuis, Wilfred den Dunnen, Harry van Goor, Jan-Luuk Hillebrands, Sergio H. Triana, Theodore Alexandrov, Marie-Cherelle Timm, Bartholomeus T. van den Berge, Martijn van den Broek, Quincy Nlandu, Joelle Heijnert, Eric M.J. Bindels, Remco M. Hoogenboezem, Fieke Mooren, Christoph Kuppe, Pascal Miesen, Katrien Grünberg, Ties Ijzermans, Eric J. Steenbergen, Jan Czogalla, Michiel F. Schreuder, Nico Sommerdijk, Anat Akiva, Peter Boor, Victor G. Puelles, Jürgen Floege, Tobias B. Huber, The COVID Moonshot consortium, Ronald P. van Rij, Ivan G. Costa, Rebekka K. Schneider, Bart Smeets, and Rafael Kramann

Supplementary Materials - Figures and Tables

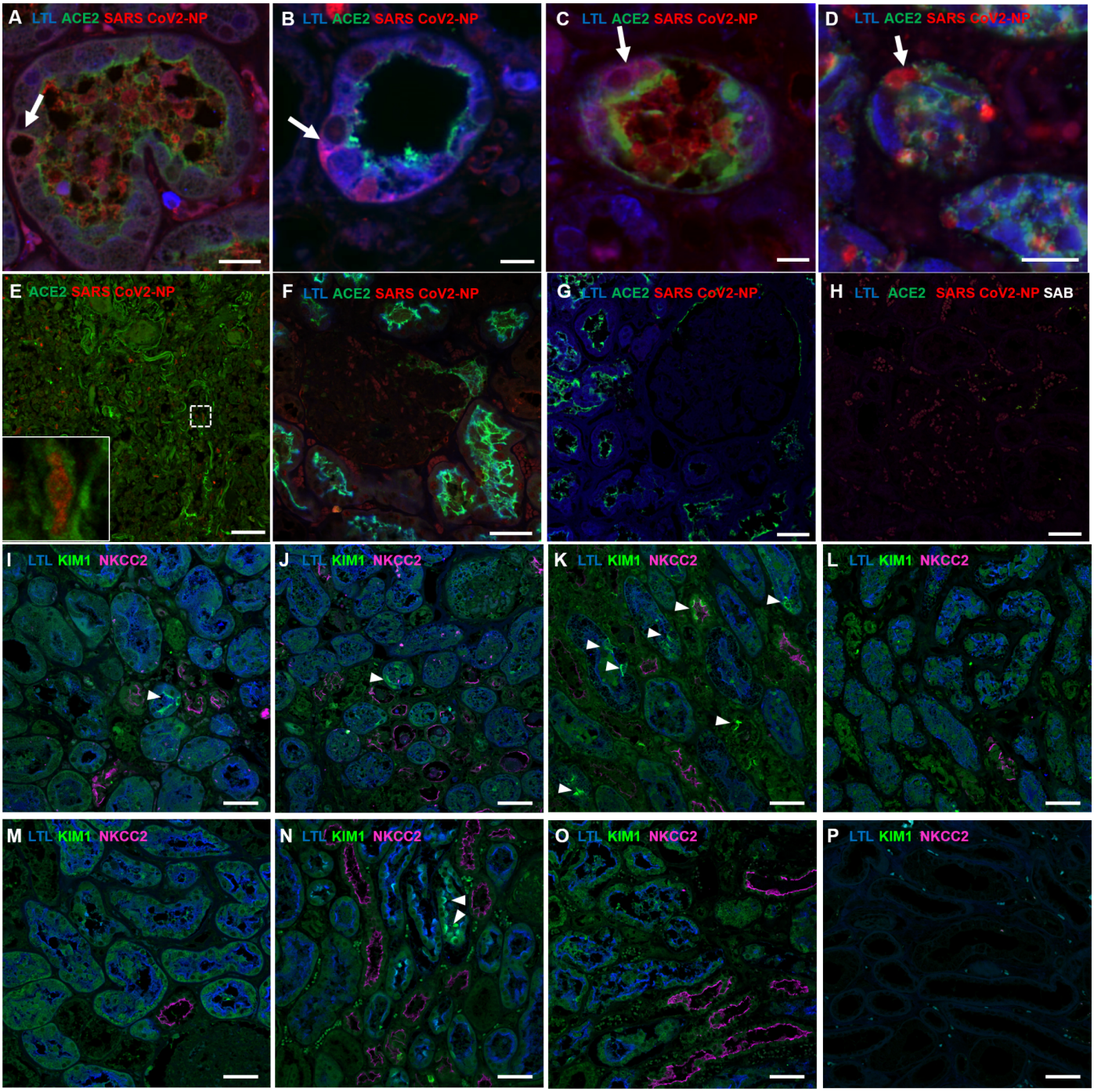

Figure S1, related to Figure 1. Additional COVID-19 patient and control kidney SARS-CoV-2 nucleocapsid and KIM1 stainings. (A-D) SARS-CoV-2 nucleocapsid (red, arrow), ACE2 (green) and LTL (blue) expression in human autopsy kidney tissue derived from four different patients. Scale bar A, D 20 µm. Scale bar B, C, 10 µm. (E) SARS-CoV-2 nucleocapsid (red) and ACE2 (green) expression in human autopsy lung tissue. (F) Human non-COVID-19 nephrectomy kidney tissue and (G) autopsy kidney tissue control stained against SARS-CoV-2 nucleocapsid (red), ACE2 (green) and LTL (blue) (H) second antibody controls (SAB). (I-M) Kidney injury molecule-1 (KIM1), LTL and NKCC2 expression in human autopsy kidney tissue derived from 5 different COVID-19 patients. (N-O) Human non-COVID-19 autopsy kidney tissue controls stained against KIM1, LTL and NKCC2. (P) secondary antibody controls (SAB). Scale bars 50 µm.

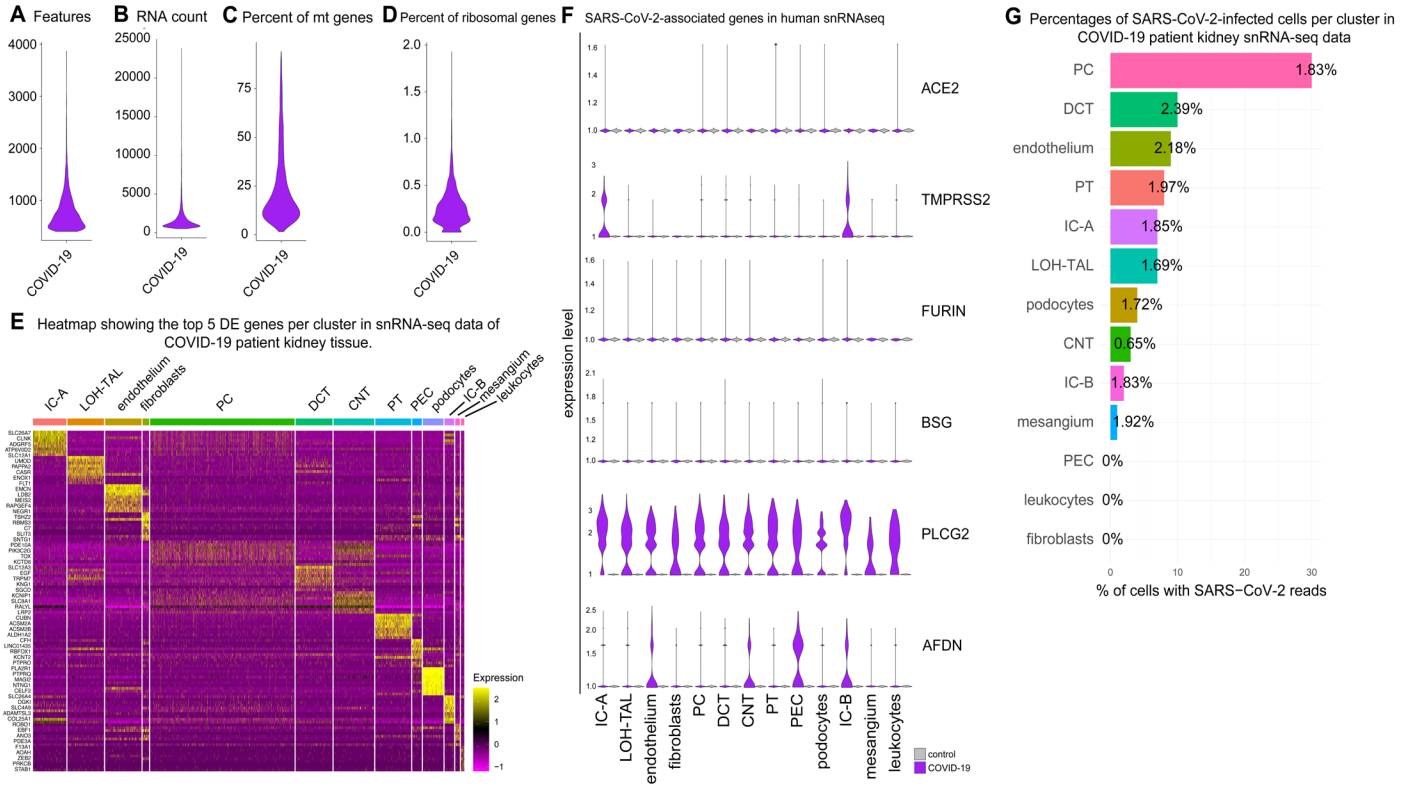

Figure S2, related to Figure 2. COVID-19 snRNA-seq dataset characteristics and SARS-CoV-2 entry factor expression in COVID-19 kidney tissue. (A-D) snRNA-seq data quality plots. (E) Heatmap depicting the top 5 DE genes per cluster in COVID-19 patient snRNA-seq data. The top 20 DE genes are listed in Table S2. (F) Violin plots showing SARS-CoV-2 cell entry factors ACE2, TMPRSS2, Furin, and BSG, as well as SARS-CoV-2-related genes PLCG2 and AFDN per cluster in snRNA-seq data of COVID-19 patient kidney tissue. (G) Percentage of SARS-CoV-2-infected cells per cluster in the COVID-19 patient kidney tissue. Data are derived from one COVID-19 patient kidney biopsy specimen.

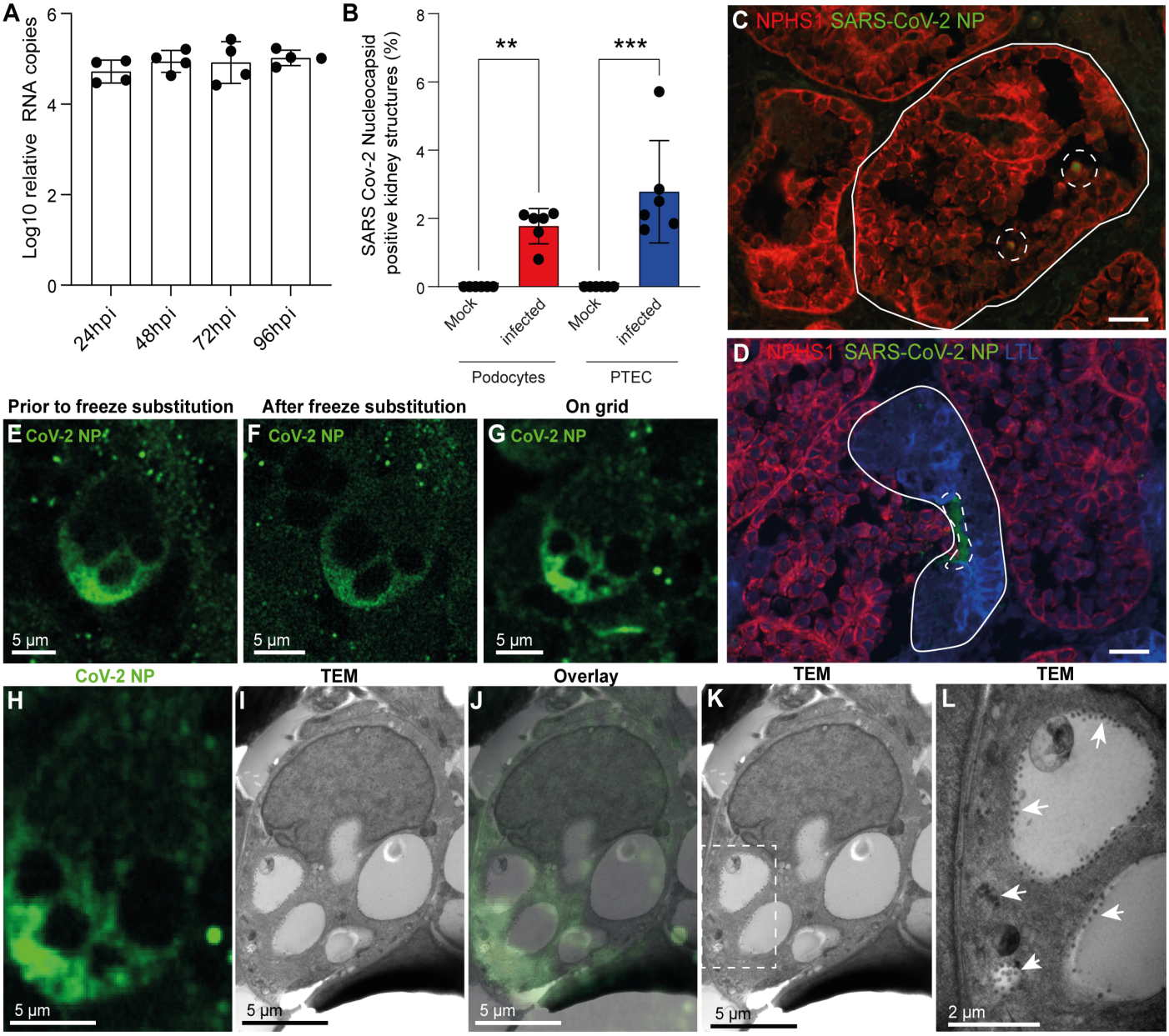

Figure S3, related to Figure 3. Viral transcript detection over time and SARS-CoV-2 nucleocapsid protein quantification in organoids and Immuno-based correlative light microscopy and electron microscopy pipeline of a SARS-CoV-2 infected cell. (A) Viral transcripts were detected 24, 48, 72, and 96 hours post infection (hpi) in kidney organoids. Data are mean and SD from 2 independent experiments each performed with 2 biological replicates. (B) Scoring of SARS-CoV-2 nucleocapsid protein expression in podocytes and proximal tubules. At least 80 podocyte clusters and proximal tubules per sample were manually scored. Data are mean and SD from 3 independent experiments each performed with 2 biological replicates. ** = $p<0.01$, *** = $p<0.001$. (C-D) Representative images of (C) one infected podocyte (NPHS1, red) cluster (white solid line) and (D) one proximal tubule (LTL, white solid line) as shown by SARS-CoV-2 nucleocapsid protein expression (green, white dashed line). Scale bar 20 µm. (E-F) SARS-CoV-2 nucleocapsid protein fluorescent signal detection (green) in a mesenchymal cell using confocal microscopy (E) prior to and (F) after high-pressure freezing followed by freeze substitution. (G) Fluorescent imaging of the organoid section containing the infected mesenchymal cell on the transmission electron microscopy (TEM) grid. The fluorescent image and the TEM image are from the same cell, but a different focal plane. (H) The SARS-CoV-2 nucleocapsid protein fluorescent signal matches the (I) corresponding ultrastructure analysis, as shown in the (J) overlay. (K-L) Viral particles are shown in vacuoles (arrows).

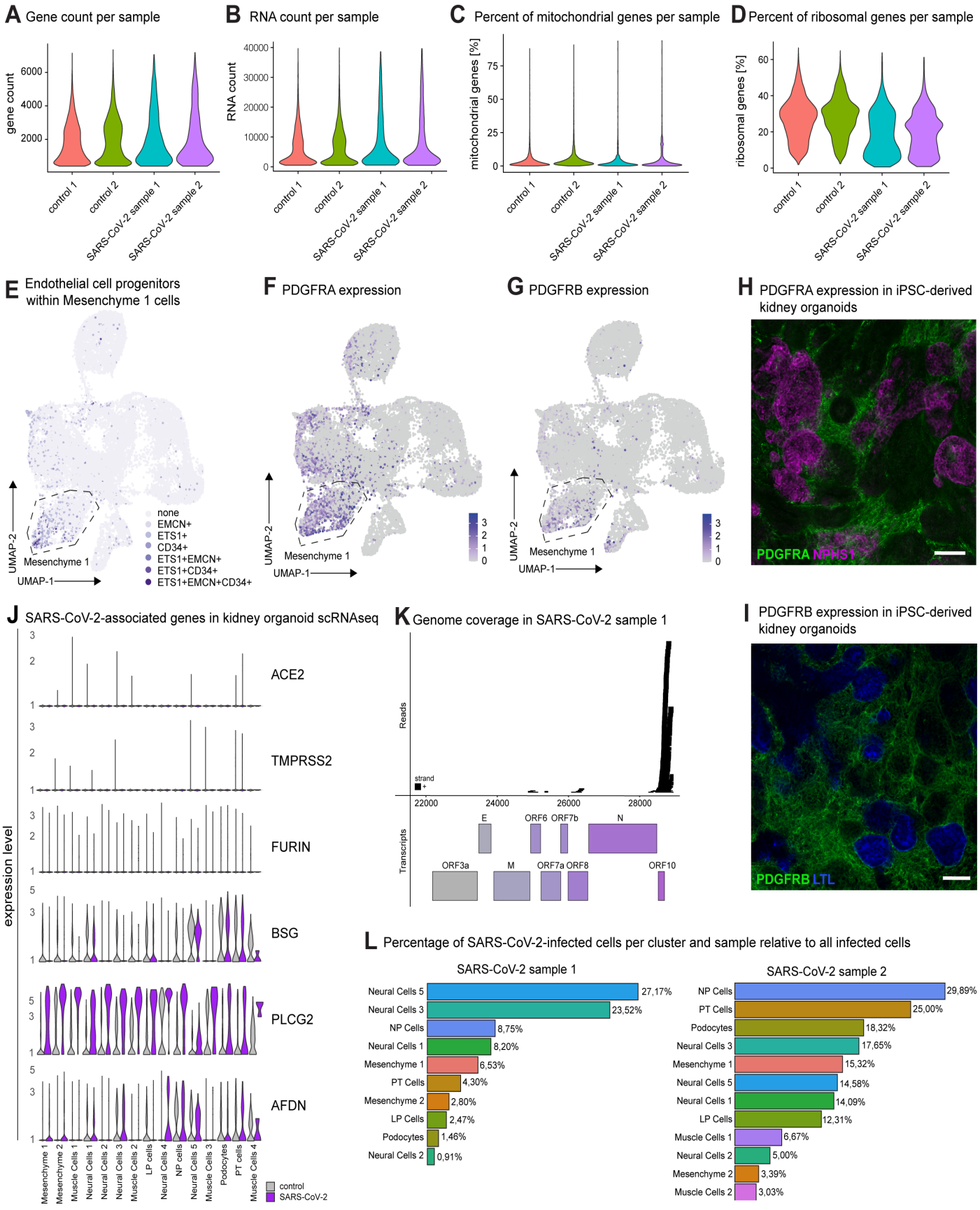

Figure S4, related to Figure 4. Supplementary data for scRNA seq of iPSC-derived kidney organoids. (A-D) Quality control data of scRNA seq data from organoids: (A) Number of genes detected in each cell per sample. (B) Total number of RNA detected within a cell per sample. Percentage of (C) mitochondrial and (D) ribosomal genes per sample. (E-G) Endothelial cell progenitors and PDGFRa/b+ cell population in organoids: (E) Endothelial cell progenitors (CD34+ETS1+EMCN+(Uhlén et al., 2015)) are present in mesenchyme cell cluster 1. (F) PDGFR alpha and (G) beta expression in kidney organoids. PDGFRa/b+ fibroblast population is most pronounced in mesenchyme cell cluster 1. (H) PDGFRa (green, interstitial compartment) and Nephrin 1 (NPHS1, purple, podocytes) protein expression in iPSC-derived kidney organoids. (I) PDGFRb (green, interstitial compartment) and LTL (blue, proximal tubules) protein expression in iPSC-derived kidney organoids.

(J) Violin plots illustrating the expression of ACE2, TMPRSS2, Furin, BSG, PLCG2, and AFDN per cluster in control and SARS-CoV-2-infected kidney organoids. (K) Virus genome coverage plot in SARS-CoV-2 sample 1. (L) Percentage of SARS-CoV-2 infected cells per cluster and samples SARS-CoV-2 1 and SARS-CoV-2 2. The respective percentages per cluster represent proportions of virus mapped cells. Data are derived from one scRNA sequencing experiment. A total of eight separate kidney organoids were pooled in one sample. Two mock-infected control samples and two SARS-CoV-2-infected samples were used as input for scRNAseq.

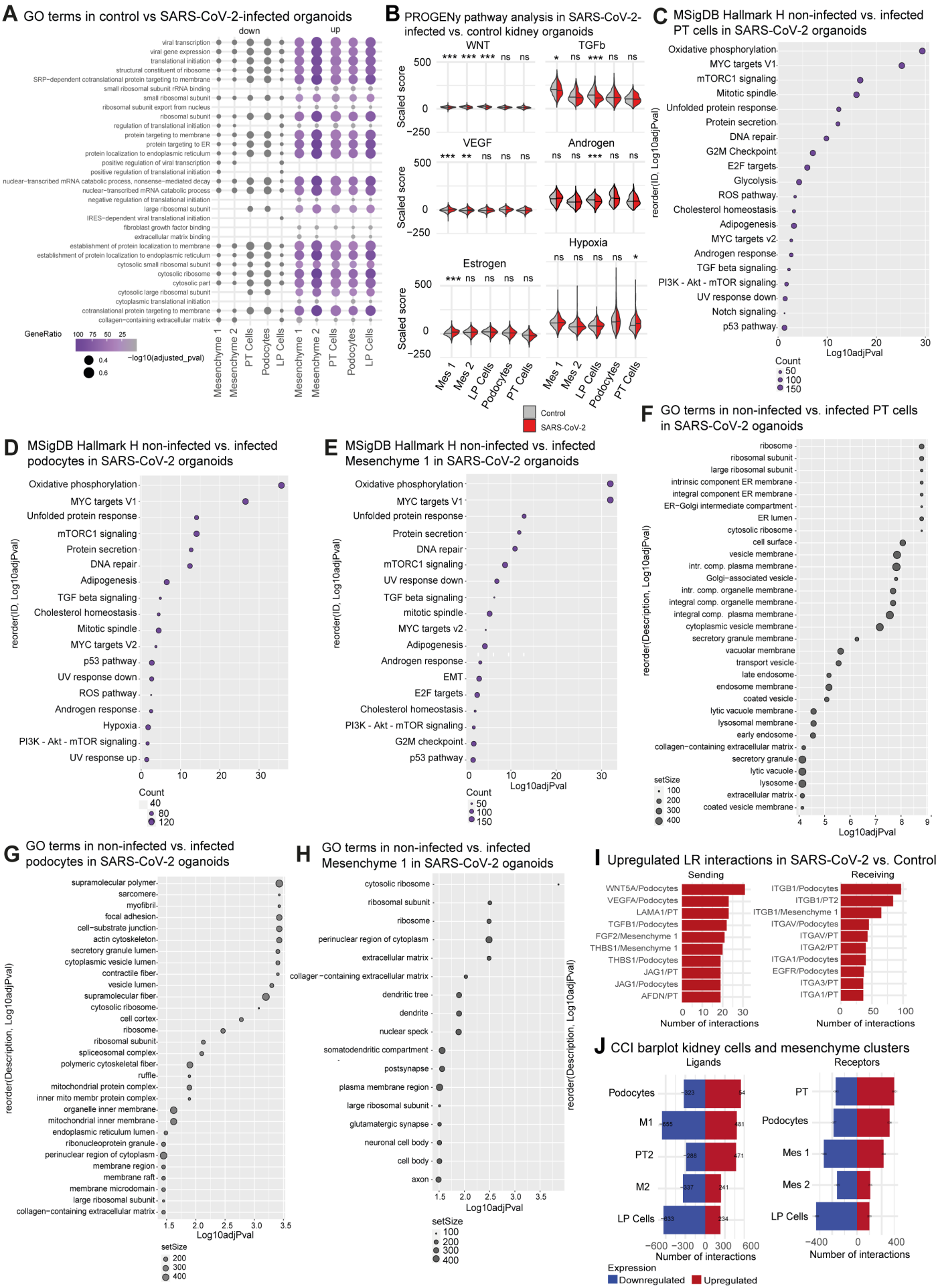

Figure S5, related to Figure 5. Additional GO terms, PROGENy, MSigDB Hallmark pathway activity and Ligand-receptor interaction profiling of SARS-CoV-2-infected human iPSC-derived kidney organoids. (A) GO terms analysis showing up- and downregulation of virus infection and processing related pathways upon SARS-CoV-2 infection of kidney organoids. (B) PROGENy analysis showing Wnt, TGFb, Hypoxia, VEGF,

Androgen, and Estrogen pathway activity in Mesenchyme clusters (Mes 1, Mes 2) and kidney epithelial cells. * = p<0.05, ** = p<0.01, *** = p<0.001. (C-E) MSigDB Hallmark analysis providing evidence of upregulation of virus infection-related cellular target upregulation in (C) proximal tubular cells, (D) podocytes, and (E) mesenchyme 1. (F-H) GO terms analysis comparing infected vs. non-infected cells per cluster in (F) proximal tubular cells, (G) podocytes, and (H) mesenchyme 1. (I) Barplot showing all up and downregulated ligand-receptor pairs in the kidney - and mesenchyme clusters. (J) Cell-cell interaction bar plot showing the total number of up and downregulated ligand-receptor pairs in the kidney - and mesenchyme clusters. Data are derived from one scRNA sequencing experiment. A total of eight separate kidney organoids were pooled in one sample. Two mock-infected control samples and two SARS-CoV-2-infected samples were used as input for scRNAseq.

Supplementary Tables

Table S1, related to Figure 1. Characteristics and corresponding statistics for the COVID-19 and control patients' cohorts.

	Cohorts			Statistical analysis			
Parameter	**control**	**ARDS**	**COVID-19**	**control *vs.* COVID-19**	**ARDS *vs.* COVID-19**	**control *vs.* ARDS**	**test applied**
Age [years]*	79.0 (±16)	54.5 (±15.5)	73.0 (±17.5)	ns	p<0.001	p<0.001	Mann-Whitney U test
male [count]	29	6	47	ns	ns	ns	χ^2 test
female [count]	14	8	15				
CKD (%)	55,8	14,2	30,6	p<0.001	ns	p<0.001	χ^2 test
Hypertension (%)	44,2	57,1	51,6	p=0.003	ns	ns	χ^2 test
Diabetes (%)	18,6	0	27,4	p=0.004	p=0.047	p=0.007	χ^2 test

*Median ± interquartile range

Table S2, related to Figure 2. Top 20 differentially expressed genes per cluster in the COVID-19 tissue specimen.

Rank	Principal cells	PTEC	LOH-TAL	DCT	IC-A	IC-B	PEC	CNT	EC	Mesengial cell	Podocytes	Leucocytes	Fibroblasts
1	ATP1B3	PDK4	AC012593.1	CALCR	UNC5D	AL136962.1	PDK4	RGS6	PDE3A	AC096577.1	AC096577.1	LEF1	IGF1
2	NR4A1	LINGO2	EGF	TRPM7	CA8	ACSM2B	NR4A1	DEFB1	AC096577.1	DHFR	EGR1	NR4A1	ADAMTS3
3	GDF15	AFF2	TIPARP	ADGRL3	PPM1E	AC096577.1	ZFP36	AC092691.1	ACSM2B	SLC4A4	MSRB3	IL7R	SYT1
4	AC087379.2	MID1	VTCN1	LINC01828	AC013472.2	ACSM2A	ATP1B3	SNTG1	ACSM2A	MT1E	PAMR1	RGS2	GREB1L
5	PDE10A	LRRC7	PCK1	SLC12A3	MSRA	CCBE1	KLHL13	AC004784.1	MT2A	NRXN3	WDR49	RNF212B	PLPP1
6	SLC45A4	PROC	CMTM8	ROBO2	NTN4	GADD45B	AC096577.1	GADD45B	AC007319.1	THBS1	AC008264.2	PIK3R5	SLC22A3
7	RALYL	FRY	FGL2	AC004870.4	FTH1	LRP2	SNAP25	BBOX1	SULF1	SLC12A1	KALRN	TSPAN5	LINC02388
8	AC004784.1	DGKG	RIPOR1	FAM20C	RUNX1	FYN	FGF14	CLSTN2	COL8A1	RCAN2	AC009975.1	SLC22A6	CLIC5
9	PGM5	CYP4A11	LINC01482	LINC01482	AC092650.1	CFTR	NAMPT	PTCHD4	EMP1	LGR6	MID1	ACSM2A	PCDH11X
10	ZFP36	NECAB1	SCNN1G	KSR2	AC098829.1	PTPRQ	VCAM1	HSPA5	FTCD	ACSM2A	ANXA1	ATP10A	NFATC2
11	PACRG	CREB5	ATP6V0A4	UBE2D2	SLC12A3	SDK2	NXN	ST6GAL1	NAV3	CLNK	PCDH9	ADAMTSL1	LINC00924
12	MAGI1	HSP90AA1	BBOX1	ABTB2	HSP90AA1	LAMA2	ACSS2	KCTD8	SIPA1L2	RBFOX1	ESRRG	NAV2	HGF
13	FGF13	PLCG2	CCDC178	DEPTOR	EFNA5	CPEB4	SLIT2	LINC00278	ADAMTSL1	CPE	TMEM117	GPAM	PWRN1
14	GALNT17	AKAP12	LRRK2	SLC8A1	TOX	MTRNR2L12	COL4A3	MT-ATP8	NCOA7	ACER2	ADAMTS19-AS1	TTN	LINC00989
15	ARHGAP18	SAMD4A	UBE2D2	MYO1E	GALNTL6	MT-ATP8	AL022068.1	SOX5	ADGRB3	KCNIP4	COBLL1	CD36	PDE1C
16	ITGA6	ITGB8	DEPTOR	MIR4435-2HG	MAGI2	SGCD	HMGCS1	LTBP1	MTRNR2L8	NRG3	MECOM	ZFPM2	ABCA8
17	ATP6V0D2	NRG1	AC019197.1	NRP1	LINC01320	ATP6V1C2	KCNIP4	PRKAG2	ST6GAL1	SEMA5A	PCDH7	MIR99AHG	ACSS2
18	RCAN2	DCC	AC024022.1	ARL15	CCSER1	ASTN2	PTPRD	LINC01482	ETS1	P4HA1	KCNIP4	IGFBP7	ARHGAP15
19	SLC26A7	DLGAP1	PLCG2	HSP90AA1	SLC8A1	AC138305.1	FMN2	LINC01320	FLRT2	SLC2A3	LRP1B	KALRN	GPAM
20	CLNK	COL4A1	SLC8A1	PRKG1	KCNIP4	KCNMB2	PLCG2	NLGN1	HSP90AA1	HSP90AA1	SLC8A1	PLPP1	NEGR1

Table S3, related to Figure 4. Top 20 differentially expressed genes per cluster in the kidney organoids.

rank	Mesenchyme 1	Mesenchyme 2	PT Cells	Podocytes	LP Cells	Neural 1	Neural 2	Neural 3	Neural 4	Neural 5	NP Cells	Muscle 1	Muscle 2	Muscle 3	Muscle 4
1	COL3A1	PAX7	SPP1	MAFB	TOP2A	**RSPO3**	ZIC2	STMN2	STMN2	**PTN**	**NHLH1**	USP18	ACTC1	TTN	ACTC1
2	**COL1A1**	TCEAL9	GSTP1	ITM2B	CENPF	MSX1	**NFIA**	**STMN4**	**DUSP8**	SOX2	STMN2	**MYOG**	MYH3	**MYH3**	TNNC2
3	OGN	**PITX2**	**KRT18**	MAGI2−AS3	**HMGB2**	ZIC2	RMST	**CRABP1**	**JUN**	**FABP7**	**NEUROD1**	**CDKN1C**	**ACTA1**	**NEB**	**MYL1**
4	LGALS1	FRMD4A	**EPCAM**	**NPHS2**	**UBE2C**	**SOX2**	**GRID2**	TUBB3	ANK3	CCND1	TUBB3	KLHL41	TNNC2	TNNC2	MYLPF
5	COL12A1	RRBP1	FXYD2	**PODXL**	MKI67	ID4	MSX1	TUBB2B	STMN4	CALR	INSM1	HSPA1A	**TTN**	MEF2C	MYH3
6	PRRX1	CLCN5	DCDC2	ANXA1	ASPM	LYPD1	AEBP1	TUBA1A	NRXN1	PTPRZ1	SOX11	MYOD1	TNNI2	TNNT1	TNNI1
7	SFRP2	PDGFA	APOE	PTPRO	PRC1	ID2	NEAT1	JUN	GRIA2	TTYH1	CACNA1A	RBM24	MYL1	ANKRD36C	ACTA1
8	COL5A2	TBX1	MT−CO3	S100A6	TPX2	RFX4	PREX1	RTN1	RAPGEF6	EDNRB	ENC1	PDLIM3	MYLPF	TNNT2	TNNI2
9	COL1A2	**FGFR4**	S100A9	WT1	HIST1H4C	ZNF503	EFNB2	GAP43	TUBA1A	IGFBP5	PHLDA1	ALPK2	TNNI1	NEXN	TPM2
10	NUPR1	PDGFC	FTL	MME	UBE2S	CCN2	ZNF503	MLLT11	CACNA1A	NTRK2	MAP1B	ZNF106	IL17B	MYLPF	KLHL41
11	VCAN	SPATS2L	KRT19	RASSF8	CKS2	TMEM47	CCN2	KIF5C	CLASP2	IFITM3	BASP1	RGS2	MYBPH	TRDN	IL17B
12	AKAP12	SIX1	MT−ND3	GADD45A	CDK1	WLS	SLC5A3	CD24	KIF5C	HSP90B1	SOX4	RASSF4	TNNT2	ACTA1	TNNT2
13	COL6A3	TAF1D	S100A6	CLIC5	NUSAP1	HOXD4	RFX4	BSCL2	NCAM1	SPARCL1	TUBA1A	SOX8	TPM2	MYL1	TTN
14	MGP	HSPA1B	ALDH1A1	BST2	SMC4	EFNB2	MED13L	GPM6A	MIAT	HSPA5	TAGLN3	PRDX6	COL19A1	RYR1	DES
15	ITM2A	NRK	MT−CO2	SQSTM1	PTTG1	PTN	MIR99AHG	BASP1	PLCG2	IGFBP2	SSTR2	EFHD2	NEXN	MYBPH	COL19A1
16	LUM	COL1A2	TAGLN	SERPINE2	CDC20	ZFP36L1	LINC00472	MAP1B	NOVA1	PPIB	TUBB2B	HSPB1	DES	TNNI1	ZNF106
17	**PDGFRA**	PLCG2	MT−ND6	TGFBR3	ARL6IP1	ZIC5	MT−CO1	NSG2	ACAP3	ITPRID2	NRXN1	PLS3	TNNT1	TNNT3	MYOG
18	COL6A2	ATAD5	EMX2	FTL	CCNB1	EPB41L4A−AS1	MALAT1	DUSP8	RTN1	MDK	TOX3	FNDC5	SMPX	MYH8	PRDX6
19	CPE	SOX8	LAMA1	VEGFA	KPNA2	ID1	ADGRV1	NRN1	CRABP1	SAT1	POU4F1	VGLL2	CRYAB	MACF1	MYBPH
20	COL4A2	IGFBP5	MPC2	MXRA8	PLK1	SLC3A2	XPO1	GNG3	TUBB3	PDIA3	RGS10	CHRNB1	TNNT3	TNNI2	HSPB2

Table S4, related to Figure 4. Viral reads and percentage of infected cells per cell type per organoid sample.

	Cluster	viral reads SARS-CoV-2 s1	virus-infected cells SARS-CoV-2 s1	total cell numbers per cluster SARS-CoV-2 s1	% of infected cells per cluster s1	viral reads SARS-CoV-2 s2	virus-infected cells SARS-CoV-2 s2	total cell numbers per cluster SARS-CoV-2 s2	% of infected cells per cluster s2
1	Mesenchyme 1	21	12	199	6.03	26	10	222	4.50
2	Mesenchyme 2	4	4	107	3.74	3	3	118	2.54
3	PT Cells	3	2	93	2.15	2	2	92	2.17
4	Podocytes	7	4	137	2.92	2	1	131	0.76
5	LP Cells	0	0	81	0.00	8	3	65	4.62
6	Neural Cells 1	35	15	256	5.86	144	13	220	5.91
7	Neural Cells 2	19	5	219	2.28	22	5	220	2.27
8	Neural Cells 3	1	1	85	1.18	22	1	102	0.98
9	Neural Cells 4	0	0	44	0.00	0	0	34	0.00
10	Neural Cells 5	18	11	92	11.96	31	7	96	7.29
11	NP Cells	8	3	80	3.75	2	2	87	2.30
12	Muscle Cells 1	0	0	29	0.00	2	1	30	3.33
13	Muscle Cells 2	0	0	8	0.00	1	1	33	3.03
14	Muscle Cells 3	0	0	22	0.00	0	0	24	0.00
15	Muscle Cells 4	0	0	2	0.00	0	0	1	0.00
	all cells	116	57	1454		265	49	1475	

S1: Organoid sample 1, S2: organoid sample 2.

Table S5, related to STAR Methods section CLEM. Freeze substitution protocol used during the CLEM sample preparation.

Step	Tstart (°C)	Tend (°C)	Slope	Time	Reagent	Conc.	Transfer	Pause	UV
1	-90	-90	0	4:00	Fs cocktail	100%	Stay		
2	-90	-45	5	9:00	Fs cocktail	100%	Stay		
3	-45	-45	0	5:00	Fs cocktail	100%	Stay		
4	-45	-45	0	0:10	Acetone	100%	Exchange		
5	-45	-45	0	0:10	Acetone	100%	Exchange		
6	-45	-45	0	0:10	Acetone	100%	Exchange		
7	-45	-45	0	2:00	R221/acetone	25%	Exchange		
8	-45	-45	0	2:00	R221/acetone	50%	Exchange		
9	-45	-30	7.5	2:00	R221/acetone	75%	Exchange		
10	-30	-30	0	12:00	R221	100%	Exchange	X	
11	-30	-30	0	2:00	R221	100%	Exchange		
12	-30	-30	0	48:00:00	R221	100%	Stay		X
13	-30	20	5	10:00	R221	100%	Stay		X
14	20	20	0	48:00:00	R221	100%	Stay		X